Published in final edited form as:

Stem Cells. 2012 July ; 30(7): 1496–1508. doi:10.1002/stem.1112.

Elf5 Regulates Mammary Gland Stem/Progenitor Cell Fate by Influencing Notch Signaling

Rumela Chakrabarti[a,b], **Yong Wei**[b], **Rose-Anne Romano**[a], **Christina DeCoste**[b], **Yibin Kang**[b], and **Satrajit Sinha**[a]

[a]Department of Biochemistry, Center of Excellence in Bioinformatics and Life Sciences, State University of New York at Buffalo, Buffalo, New York, USA

[b]Department of Molecular Biology, Princeton University, Princeton, New Jersey, USA

Abstract

The transcription factor E74-like factor 5 (Elf5) functions downstream of the prolactin receptor signaling pathway and plays an important role in mammary gland development. Using conditional mouse knockouts, we have previously shown that Elf5-null mammary glands exhibit a complete failure of alveologenesis during pregnancy. The Elf5-null developmental phenotype is mediated through alteration in the expression of several critical genes involved in alveologenesis, particularly those belonging to the JAK/STAT pathway. Here, we demonstrate that in addition to regulating terminal differentiation of alveolar cells, Elf5 also plays a critical role in determining cell fate and in regulating the stem/progenitor function of the mammary epithelium. Targeted deletion of Elf5 in the mammary glands leads to accumulation of cell types with dual luminal/basal properties such as coexpression of K8 and K14 and an increase in $CD61^+$ luminal progenitor population during pregnancy. Further interrogation suggests that the abnormal increase in $K14^+K8^+$ cells may represent the $CD61^+$ luminal progenitors blocked in differentiation. Remarkably, Elf5 deficiency in mammary epithelium also triggers an increase of adult mammary stem activity as evidenced by the accumulation of mammary stem cell (MaSC)-enriched cell population in both pregnant and virgin mice and further confirmed by mammosphere and transplantation assays. Additional support for this phenotype comes from the enriched MaSC gene signature based on transcriptomic analysis of the Elf5-null mammary gland. Finally, our biochemical studies suggest that Elf5 loss leads to hyperactivation of the Notch signaling pathway, which might constitute in part, the underlying molecular mechanism for the altered cell lineage decisions in Elf5-null mammary epithelial cells.

Correspondence: Rumela Chakrabarti, Ph.D., Department of Molecular Biology, Princeton University, Princeton, New Jersey 08554, USA. Telephone: 330-389-1943; Fax: 609-258-2340; rchakrab@princeton.edu; or Satrajit Sinha, Ph.D., Department of Biochemistry, State University of New York, Center of Excellence in Bioinformatics and Life Sciences, 701 Ellicott Street, Buffalo, New York 14203, USA. Telephone: 716-881-7994; Fax: 716-849-6655; ssinha2@buffalo.edu.

Author contributions: R.C.: conception, design, collection of data, analysis, and manuscript writing; Y.W.: technical support and analysis; R.R.: technical support; C.D.: collection of data; Y.K.: manuscript writing; S.S.: conception, analysis, and manuscript writing.

Disclosure of Potential Conflicts of Interest

The authors indicate no potential conflicts of interest.

See www.StemCells.com for supporting information available online.

Keywords

Elf5; Mammary gland; Alveologenesis; Mammary stem cells; Notch; Knockout

Introduction

The adult mammary gland is an epithelial-rich organ that undergoes remarkable structural and physiological changes during pregnancy. The main structures that are primarily affected by these dynamic changes at this stage are the milk-producing alveoli and the elaborate ductal network. The epithelial lining of the alveoli and the ducts comprises two major cell types: luminal and basal [1, 2]. The generation of the mature and functional lobuloalveolar units of the mammary gland during pregnancy is governed by endocrine signals generated predominantly by prolactin and steroid hormones such as progesterone and a network of critical transcription factors that activate target genes involved in cell-fate determination, proliferation, and differentiation [3–5]. One such transcription factor is E74-like factor 5 (Elf5, also known as ESE-2).

Elf5 is highly expressed in tissues rich in glandular or secretory epithelial cells such as mammary gland, salivary gland, kidney, lung, and stomach [6–10]. In addition, during early embryonic development, Elf5 expression is restricted to the extraembryonic ectoderm, which is essential for mammalian placental formation and the survival of the embryo in utero [11]. Elf5 is a critical transcription factor at this stage, since Elf5-null embryos die early during embryogenesis and exhibit defects in the formation of extraembryonic ectoderm [6, 11, 12]. Indeed, recent studies have shown that Elf5 is important for the maintenance of the trophoblast stem cell population and is differentially and epigenetically regulated to dictate embryonic and trophoblast cell lineage choices [13].

In mammary glands, Elf5 is highly induced during pregnancy and is primarily restricted to the luminal epithelial cells [12, 14, 15]. The important role of Elf5 in mammary gland development is clearly evident in the lactation failure and blocked alveolar morphogenesis phenotype in Elf5 females, even under heterozygous conditions [12, 16]. The importance of Elf5 in lactation is further exemplified by the precocious alveolar differentiation phenotype observed in Elf5-overexpressing virgin mammary glands [16]. These studies have firmly established this transcription factor as a master regulator of the alveolar switch. To overcome the problem of embryonic lethality of mice lacking Elf5, we have used the Cre-loxP system to ablate Elf5 specifically in the mammary epithelium [14]. We have shown that conditional loss of Elf5 in mammary glands leads to a complete failure in lobuloalveologenesis and alterations in the PrlR/Janus Kinase2/Signal transducers and activators of transcription 5a signaling pathway as well as many other known mediators of the mammary gland developmental program suggesting a much broader role of Elf5 [14, 17, 18]. Indeed, recent studies on transcriptional mediators of stem/progenitor cell differentiation and lineage control mechanisms of mammary epithelial cells (MECs) have unearthed the role of key players such as GATA-3 and to some extent Elf5 in these processes [16, 19, 20].

While animals lacking GATA-3 exhibit morphogenetic block during mammary placode formation and pubertal mammopoiesis, Elf5-null mammary glands examined so far do not

exhibit any early developmental defects in ductal growth and morphogenesis [16, 19, 20]. However, pregnant Elf5-null glands harbor an expanded pool of luminal progenitor cells suggesting that Elf5 might actively influence the dynamics of mammary epithelial progenitors and their programmed differentiation [16]. Given the broad expression pattern of Elf5 that extends beyond the pregnancy/lactation window and the emerging evidence that Elf5 is a prototypic marker for both human and mouse luminal progenitor population, it is conceivable that this factor may also influence earlier stages of the mammary epithelial lineage choices [21].

In this study, we used the Elf5 conditional knockout animals to further understand the underlying molecular mechanism by which Elf5 dictates cell-fate determination and lineage choices in mammary gland development. Our data show that loss of Elf5 leads to an unexpected and dramatic increase in $K14^+/p63^+/K8^+$ mixed population of cells in the luminal compartment, suggesting an increased progenitor cell population. Flow cytometric analysis also revealed an increase in $CD61^+$ cells during pregnancy in agreement with previous studies [16]. Interestingly, sorted $CD61^+$ subpopulations showed an increase of double-positive $K14^+/K8^+$ cells in Elf5-null MECs, suggesting that the $CD61^+$ fraction might represent cells with dual characteristics that are blocked in differentiation toward mature luminal cells. Furthermore, we also observed an increase of mammary stem cells (MaSCs) in the absence of Elf5 that is detectable during pregnancy as well as in the virgin stage. Flow cytometric analyses as well as mammosphere assays and in vivo transplantation experiments confirmed the increased stem cell activity in Elf5-null mammary glands in both pregnant and virgin stage. Finally, our findings that loss of Elf5 leads to hyperactivation of Notch signaling and that inhibition of Notch signaling can partly restore the increased stem/progenitor cell activity of Elf5-null MECs provide a novel mechanistic link between Elf5 and Notch signaling pathway in mammary gland development.

Methods and Materials

Animal Studies

The Elf5-null mice have been described previously [14]. Mice of C57BL/6 strain (6–8 generations) were used for experiments with virgin mammary glands. The genotype of the control wild-type (WT) animals was either K14-Cre/$Elf5^{+/+}$ or $Elf5^{f/f}$, whereas the genotype of the Elf5 conditional knockouts (Elf5-null) was K14-Cre/$Elf5^{f/f}$. Animal procedures were conducted in compliance with the guidelines of the IACUC Committee of the State University of New York at Buffalo.

Histological Analysis, Immunostaining, and Western Blots

For histological analysis, mammary gland specimens were fixed as described in [14]. Antibodies dilutions used for immunofluorescence and immunohistochemistry are described in Supporting Information Table S1. Protein extracts were prepared and Western blot was performed as described in [14]. Antibodies used for Western blot are described in Supporting Information Table S1.

Primary MEC Culture and Viral Infection

Isolation and adenoviral transduction of primary MECs were performed as described previously [14, 22]. For lentiviral mediated knockdown studies, shRNA knockdown vector for murine Rbpjk/Cbf-1 (TRCN0000097287-88) was purchased from Open Biosystems Inc. (Huntsville, AL, https://www.openbiosystems.com/). Control plasmid containing empty vector was purchased from Sigma-Aldrich (St Louis, MO, http://www.sigmaaldrich.com/sigma-aldrich/home/html). Plasmids were packaged into virus using HEK293-T-cells as packaging cell lines using helper plasmids VSVG and dR8.9 using standard protocols. Primary cells were spin infected with virus-containing media supplemented with 2 μg/ml polybrene for 2 hours at 1,000*g* at 4°C and then either plated in matrigel or transplanted.

Flow Cytometry/Fluorescence-Activated Cell Sorting

Single MECs suspension was pelleted and resuspended in fluorescence-activated cell sorting (FACS) buffer (1% BSA in PBS). Briefly, MECs were blocked with anti-CD16/CD32 Fcc III/II receptor antibody (BD Pharmingen, San Jose, California, http://www.bdbiosciences.com/home.jsp) and stained with a combination of either (FITC-CD45, FITC-Ter119, FITC-CD31, CD24-PE, CD29-APC, and biotinylated-CD61) or (biotinylated-CD45, biotinylated-Ter119, biotinylated-CD31, CD24-PE, CD29-FITC, and CD61-APC) for 20 minutes on ice. FACS analysis was performed using the LSRII Flow Cytometer (BD Biosciences) and data were analyzed using FlowJo software (TreeStar, Inc.). The FACS analysis described above was repeated with five or more independent samples obtained from mammary glands number 4 and 5 of WT and Elf5-null females at P17.5d and 7-week virgin. Flow sorting was performed using FACS Aria (BD Biosciences) or FACS Vantage SE w/ DiVa (BD Biosciences).

Mammosphere and Colony-Forming Assay

For mammosphere and colony-forming assays, primary MECs isolated from mammary glands number 4 and 5 of WT and Elf5-null mice (P17.5d and 6–8 week virgin) were either plated onto six-well, ultralow attachment plates at a density of 10,000 cells per milliliter or in matrigel at a density of 1,000 or 20,000 cells, respectively. Cells were grown as described previously [23, 24]

Limiting Dilution Assay and Extreme Limiting Dilution Assay

Single-cell suspension of primary MECs from WT and Elf5-null mammary glands at 6–8 weeks were sorted in combination with the Lin^-, $CD24^+$, and $CD29^{hi}$ markers to obtain MaSCs ($Lin^-CD24^+CD29^{hi}$) that were then injected into cleared mammary fat pads. The outgrowths were analyzed at 8 weeks post-transplantation. Transplantation was performed with cells resuspended in 50% Matrigel and 50% PBS. Frequency of MaSCs in transplanted cell suspension was calculated using L-calc software (StemCell Technologies, Vancouver, Canada, http://www/stemcell.com/) or extreme limiting dilution assay (ELDA) [25]. Single-hit model was also tested using ELDA and value of slope was 1. MaSC abundances were assumed to follow a Poisson distribution in LDAs, and generalized linear models using a log-log link function were used to derive repopulation frequency parameters. Differences in repopulation frequencies (defined as the number of cells required for repopulation to be

observed 63% of the time) were determined by relying on the asymptotic normality of the maximum likelihood estimates.

Real-Time PCR Analyses

Total RNAs were isolated and real-time PCR was performed as described previously [14]. The gene-specific primer sets are listed in Supporting Information Table S2.

Gene-Set Enrichment Analysis

We used GSEA v2.0 to perform the gene-set enrichment analysis (GSEA) on various functional and/or characteristic gene signatures [26, 27]. Normalized microarray expression data were rank-ordered by differential expression between Elf5-null versus WT, using the provided ratio of classes (i.e., fold change) metric. The details of the microarray experiments will be described in a separate manuscript. Gene sets were either obtained from the MSigDB database v3.0 (SEPT 2010 release) or manually generated. Milk proteins contain a list of nine genes: *Adfp, Btn1a1, Lalba, muc1, Xdh, Wap, Csnkappa, Csn1s1, and Csnk1g2*. "CDK inhibitors" include all eight gene family members (Cdkn1a through Cdkn3); MaSC-enrich and luminal signatures are significantly upregulated genes ($p < .05$ and FC >3) in MaSC-enriched and luminal subpopulations from MECs of virgin mice, which were derived from microarray dataset GSE22446.

Results

Inappropriate Expression of Basal Markers and Expansion of $K14^+/K8^+$ Dual-Positive Cells in Elf5-Null Mammary Glands

Previously, we have shown that mammary epithelium-specific deletion of Elf5 leads to a complete block in alveologenesis during lactation [14]. To further probe the effects of loss of Elf5 during different stages of pregnancy, we compared mammary glands from K14-Cre/$Elf5^{f/f}$ (Elf5-null) animals and their K14-Cre/$Elf5^{+/+}$ (WT) type littermate controls. Both whole mount carmine staining and histological examination of mammary gland sections demonstrated that at P4.5 there were discernable morphological alterations including less tertiary branching in Elf5-null mammary epithelium (Supporting Information Fig. S1). Notably, these effects were more pronounced at later stages of pregnancy in agreement with higher expression levels of Elf5 at this stage (Supporting Information Fig. S1, S2 and [12, 15]). Immunohistochemical staining confirmed the complete absence of Elf5 protein at all stages of development in the Elf5-null mice (Supporting Information Fig. S2). To further characterize the cell population in the Elf5-null epithelium, we used a panel of basal and luminal cell markers. While $K14^+$ staining was predominantly restricted to myoepithelial cells of the basal compartment in WT (Fig. 1C, 1I, 1O), in Elf5-null tissues, there was widespread mis-expression of K14 within the cells of the luminal compartment (Fig. 1F, 1L, 1R). This distinctive altered expression pattern was clearly evident at early stages of pregnancy (yellow arrows, P4.5) and progressively increased during later stages of pregnancy and at parturition (Fig. 1L, 1R, 1X and graph below [WT = 2% vs. Elf5-null = 50%]). Importantly, the altered K14 expression in luminal cells was also detectable in 12 weeks virgin mammary glands (Supporting Information Fig. S3). However, in contrast, K5 expression was restricted to myoepithelial cells in both Elf5-null and WT type mammary

glands (data not shown). This was not surprising, given the reported asynchronous distribution of K5 and K14 during mammary gland development [28, 29]. On the other hand, immunostaining with p63, another basal cell marker, showed results similar to K14. Indeed, $p63^+$ cells were scattered throughout the luminal compartment in Elf5-null mammary epithelium (Supporting Information Fig. S4B, Fig. S4D, S4F) in comparison to the myoepithelial-restricted expression observed in WT, at multiple stages of development (Supporting Information Fig. S4A, S4C, S4E). These data are in agreement with Western blot analysis that demonstrated increase in basal markers p63 and K14 expression in Elf5-null tissue (Supporting Information Fig. S5). To further examine the nature of the $K14^+/p63^+$ cell types, we performed dual staining of K8 and K14. $K8^+$ cells were uniformly present within the luminal layer of control ducts, as expected, and were surrounded by a single layer of $K14^+$ myoepithelial cells along the ducts (Fig. 2C). In contrast, in affected areas of Elf5-null tissue, there was a robust increase of dual $K14^+/K8^+$ population (WT = 0.5% vs. Elf5-null = 44%) (white arrows, Fig. 2F). This observation was further supported by increased colocalization of p63 and K8 in the luminal compartment in P17.5 mammary glands of Elf5-null (Fig. 2L) in comparison to WT (Fig. 2I) (WT = 1.2% vs. Elf5-null = 16%). Next, we examined expression of smooth muscle actin (SMA), a marker of mature differentiated myoepithelial cells. While the outer layer of myoepithelial cells in the Elf5-null and control mammary glands displayed the normal pattern of SMA staining, the $K14^+$ population in the luminal compartment of the Elf5-null mammary glands was negative for SMA, suggesting that these mixed-phenotypic cells were un-differentiated (Fig. 2O, 2R).

Loss of Elf5 Alters Stem Cell/Progenitor Populations During Pregnancy

Given the prevailing notion that both the myoepithelial and luminal cell types are descendent of a common progenitor population that expresses dual $K14^+/K8^+$ markers, we wondered if the stem/progenitor cells were affected in Elf5-null mammary glands. To test this, we dissected mammary glands from P17.5d mice and analyzed them by flow cytometry (Supporting Information Fig. S6A) with established surface markers [24, 30]. We observed a consistent increase in $Lin^-CD24^+CD29^{hi}$ (MaSC enriched) cell population (WT = 35% vs. Elf5-null = 59.1%) and a decrease in the $Lin^-CD24^+CD29^{lo}$ population (WT = 32.5% vs. Elf5-null = 20.5%) in Elf5-null MECs compared to WT (Fig. 3A, Supporting Information S7A, S7B). The $Lin^-CD24^+CD29^{lo}$ compartment can be further subdivided into $CD61^+$ progenitor cells and $CD61^-$ differentiated mature cells [19]. Further characterization of the luminal progenitors using the CD61 marker showed significant increase in percentage of $Lin^-CD24^+CD29^{lo}CD61^+$ population in the Elf5-null mammary epithelium in comparison to WT control (Fig. 3B), similar to earlier studies [16]. The purity of the various sorted populations was confirmed by real-time RT-PCR (qRT-PCR) for K14 and K18 as shown in Supporting Information Figures S8A and S8B. We next performed dual immunofluorescence staining of the $Lin^-CD24^+CD29^{lo}CD61^+$ population for K14 and K8 expression. This showed that the $CD61^+$ Elf5-null MECs from P17.5 consists of a significantly larger (Elf5-null = 42% vs. WT = 16%) fraction of $K14^+/K8^+$ cell population compared to the WT (double-positive cells are marked by yellow arrowheads in Fig. 3C and bar graph in Fig. 3D). Taken together, these data suggest that in the conditional Elf5 knockout mammary glands, the alveolar differentiation block is also accompanied by accumulation of premature cells that might represent stem/progenitor fractions.

We next examined the functional effects of loss of Elf5 on stem/progenitor population proliferation and expansion by mammosphere and colony-forming assays. MECs derived from Elf5-null P17.5 mammary gland showed an increase in primary mammosphere-forming activity compared to WT cells (Fig. 3F), indicating increased stem or progenitor cell function. In addition, the mammosphere diameters were larger in Elf5-null samples in comparison to the WT (Fig. 3E, 3F). Primary mammosphere-derived cells can initiate secondary mammospheres, as well as differentiate to various breast line-ages, thus exhibiting two fundamental properties of stem cells—self-renewal and multilineage differentiation [31]. To examine self-renewal and intrinsic stem cell activity, second-generation mammospheres were counted, which revealed a distinct increase in secondary mammosphere-forming activity in Elf5-null MECs compared to the WT cells (Fig. 3G). When individual mammospheres were plated on collagen-coated chamber slides, most cells in the spheres differentiated and migrated out of the center after 4 days of culture. Immunostaining of differentiated mammospheres identified $K8^+$ and $K14^+$ cells from both WT and Elf5-null mammospheres (Fig. 3H), confirming that the spheres were capable of differentiating into both luminal and basal lineages. Of note, similar to Elf5-null mammary glands in vivo, an increase in dual-positive ($K14^+/K8^+$) cells was also observed in the differentiated cells of the Elf5-null mammospheres (Fig. 3H). We next compared the colony-forming capacity/progenitor activity of WT and Elf5-null MECs that were grown at clonal density in Matrigel and examined their potential to form spherical colonies. Elf5-null MECs formed more spherical colonies in comparison to WT per 1,000 MECs seeded (Fig. 3I, 3J). Average sphere size in Elf5-null was larger than WT; however, this increase was not statistically significant (data not shown). These results were further confirmed by examining mammosphere formation and colony-forming ability of purified sorted subpopulations from WT and Elf5-null MECs, ($Lin^-CD24^+CD29^{hi}$ and $Lin^-CD24^+CD29^{lo}$), respectively (Supporting Information Fig. S8C, S8D).

Increased Stem/Progenitor Cell Population and Activity in Elf5-Null MECs Obtained from Virgin Animals

We next examined whether loss of Elf5 also affects stem/progenitor cell population in virgin animals. Flow cytometry profile of WT and Elf5-null MECs of 7-week-old virgin animals showed an increase in MaSC-enriched $Lin^-CD24^+CD29^{hi}$ population in Elf5-null MECs compared to WT (WT = 13.3% vs. Elf5-null = 24.2%). This data suggested that Elf5 loss might initiate alterations in stem cell/progenitor cells as early as in virgin stage (Figs 4A, Supporting Information S6B, S7C). We next examined the $CD61^+$ luminal progenitor population. No significant difference was observed in the $CD61^+$ population in the Elf5-null mammary epithelium compared to WT (Fig. 4B) as reported previously [16]. Interestingly, immunostaining of $CD61^+$-sorted subpopulation with K14 and K8 antibodies demonstrated an increase in dual-positive cells in $CD61^+$ population albeit at lower frequency (Elf5-null = 1.67% vs. WT = 0.11%, Fig. 4C, 4D). We then compared the mammosphere-forming ability of WT and Elf5-null virgin MECs. There was a significant increase in primary mammosphere number between WT and Elf5-null MECs but no difference in relative sizes (Fig. 4E–4G). Next, we compared the colony-forming capacity/progenitor activity of WT and Elf5-null MECs grown at clonal density in Matrigel and counted spherical colonies. No significant difference was observed between Elf5-null MECs in comparison to WT per 1,000

MECs seeded (Supporting Information Fig. S8E) as could be expected due to an unaltered $CD61^+$ population.

To assess the ability of Elf5-null MaSCs to form an entire functional mammary gland in vivo, stem cell-enriched populations ($Lin^-CD24^+CD29^{hi}$) from 6 to 8-week-old virgin mice were transplanted into cleared fat pads of mice. MaSCs from both Elf5-null and WT mice were able to generate ductal outgrowths with primary and secondary side branches. However, limiting dilution analyses (Fig. 4H, 4I and Table 1) revealed a clear increase (~2.4-fold, p value .012) in repopulating frequency for Elf5-null cells, which contain 1 MaSC/MRU (mammary repopulating units) per 90 cells, compared to WT counterparts (one MaSC/MRU per 214 cells). In addition, estimation of outgrowths (percentage of mammary fat pad occupied by transplants) also showed a significant increase in outgrowths from Elf5-null MEC transplants compared to WT MECs transplants ($p = .0042$) (Fig. 4H, 4I).

Loss of Elf5 Is Associated with Altered Notch Signaling Pathway

To gain mechanistic insight into the underlying molecular events associated with the phenotype due to loss of Elf5, we performed microarray analysis with RNA isolated from WT and Elf5-null mammary gland. The global transcriptome changes due to loss of Elf5 were examined for enrichment of various signaling pathway target gene sets. GSEA demonstrated that, consistent with the observed phenotype of Elf5-null mammary glands [14], there was a reduction in expression levels of genes encoding for milk proteins and gap junction proteins in Elf5-null samples compared to WT (Fig. 5A). Furthermore, a large number of CDK inhibitors were upregulated in Elf5-null MECs in agreement with the reduced proliferation phenotype observed in Elf5-null mammary gland [14] (Fig. 5A). Interestingly, MaSC-enriched genes were significantly overrepresented among upregulated genes in Elf5-null mammary gland transcriptome—a feature that is consistent with the increased MaSC/progenitor activity of Elf5-null MECs as described earlier (Fig. 5A). In parallel, luminal-enriched genes were significantly overrepresented in downregulated genes in Elf5-null mammary gland transcriptome compared to WT (Fig. 5A).

Given the increasing evidence for a critical role of Notch signaling in cell-fate decisions in mammary gland, we were intrigued by the elevated expression of Notch signaling pathway components such as *Notch1*, *Notch2*, and *Hey1* in Elf5-null cells (Fig. 5B) [31–33]. In support of the microarray data, qRT-PCR analyses revealed that the expression of the majority of the critical genes (*Notch1*, *Notch4*, *Hes1*, *Hey1*, *Jag2*, *and Rbpjk/Cbf-1*) involved in Notch signaling cascade was higher in the Elf5-null mammary glands, whereas only Notch2 was downregulated (Fig. 5C). To further confirm whether these changes were specific to the epithelial cells, we next performed qRT-PCR on purified MECs from WT and Elf5-null P17.5 mammary glands. As shown in Supporting Information Figure S8F, the data again clearly demonstrated that the alterations in the expression levels of most of the genes such as *Notch1*, *Notch3*, *Notch4*, *Hey1*, *Jag1*, *Jag2*, *Dll1*, *Dll4*, and *Rbpjk/Cbf-1* were intrinsic to epithelial cell. To test whether these changes were also reflected in protein expression, we probed mammary glands from Elf5-null and control animals with antibodies against NICD1 (Notch1 intracellular domain), NICD4 (Notch4 intracellular domain), and Hey1, two important mediators of the Notch signaling. Our data showed an increase in

NICD1, NICD4, and Hey1 protein levels in Elf5-null mammary epithelium as judged by Western blot (Fig. 5D) and immunohistochemistry (Fig. 5E) further corroborating the qRT-PCR findings.

Elf5 Is Required for Notch Expression and Activation in Cultured MECs

To examine the direct role of Elf5 in regulating Notch signaling, we assessed the effects of loss of Elf5 in primary MECs. MECs were harvested from $Elf5^{f/f}$ mice and transduced with either adenovirus-expressing green fluorescent protein (GFP) (Ad-GFP) or Cre (AdCre) and cultured on Matrigel for varying time points in proliferative growth media. Infection of MECs with AdCre resulted in significant knockdown of *Elf5* expression (Fig. 5F, 5G). We performed qRT-PCR analyses of the primary cultures lacking Elf5 (Ad-Cre-$Elf5^{f/f}$) to examine the expression levels of some of genes in the Notch pathway that were altered in Elf5-null mammary glands in vivo. Interestingly, while both *Notch1* and *Notch4* transcripts were significantly upregulated in Ad-Cre-$Elf5^{f/f}$ compared to (Ad-GFP-$Elf5^{f/f}$) cells, others such as *Rbpjk/Cbf-1* did not show any significant change suggesting that some of these might reflect indirect targets of Elf5 in mammary glands (Fig. 5F). To further examine Notch activity, protein lysates were harvested from MECs and Western blots were performed. Concomitant with loss of Elf5 in AdCre-transduced $Elf5^{f/f}$ MECs (Fig. 5G), there was a strong increase in the expression of NICD1 but not NICD4, after 72 hours of Cre treatment. Thus, although acute loss of Elf5 leads to increased expression of both *Notch1* and *Notch4* mRNA in MECs, only *Notch1* alone is activated, suggesting that additional modes of Elf5-independent Notch4 regulation exist. Interestingly, the increased Notch1 expression was also detected in sorted $Lin^{-}CD24^{+}CD29^{lo}CD61^{+}$ population from Elf5-null MECs compared to WT (Fig. 5H).

The Increased Stem/Progenitor Cell Phenotype of Elf5-Null MECs can be Rescued by Attenuation of Notch Activity

The increase in MaSC activity and upregulated Notch signaling (Figs. 3, 5) might be secondary to the developmental block that leads to increased undifferentiated cells in Elf5-null pregnant mammary glands. To rule out this possibility, we next examined the expression of several of the critical genes in the Notch signaling pathway in 6–8 weeks Elf5-null virgin mammary glands (where no significant phenotypic difference was observed). qRT-PCR data showed increased expression of several of the Notch signaling genes including *Notch1*, *Notch3*, *Notch4*, and *Hes1* in the Elf5-null MECs compared to WT (Fig. 6A). This suggested that the upregulated Notch signaling in the absence of Elf5 is likely a direct effect and not merely due to a differentiation block.

We then examined the effects of specifically inhibiting Notch signaling in the Elf5-Null MECs on colony-forming ability in mammosphere assays, matrigel cultures, and in vivo transplantation assays. Disruption of the Notch pathway was achieved through pharmacological inhibition by GSI, a potent inhibitor of γ-secretase, the primary Notch cleaving and activating enzyme. Interestingly, disruption of Notch signaling via gamma secretase inhibitor (GSI) significantly reversed the increased stem/progenitor activity of the Elf5-Null MECs as demonstrated by the decreased mammosphere number (Fig. 6B) and colony numbers (Fig. 6C). Given the potential for pleiotropic effects due to GSI activity, we

next used shRNAs against Rbpjk/Cbf-1 for an independent confirmation of this finding. Robust knockdown of Cbf-1 in primary MECs was confirmed by qRT-PCR after infection with lentiviral particles containing two separate shRNAs against Cbf-1 (Fig. 6D). As observed with GSI based experiments, there was significant decrease in mammosphere number and colony numbers in shRNA-transduced Elf5-Null MECs compared to vector control transduced Elf5-Null MECs (control) (Fig. 6E, 6F), thus confirming the notion that the increase in stem/progenitor population in the absence of Elf5 is dependent upon increased Notch signaling. To extend these studies further, we inhibited Notch signaling in the purified $Lin^{-}CD24^{+}CD29^{hi}$ cell population using both GSI and Rbpjk/Cbf-1 shRNAs. Similar to the results obtained using unpurified MECs, we noted a decrease in number of colonies in the enriched MaSC population treated with GSI or with shRNAs that targeted Cbf-1 (Fig. 6G, 6H). We next performed transplantation assay with limiting number (100 cells per transplant) of $Lin^{-}CD24^{+}CD29^{hi}$ cells transduced with Cbf-1 targeting shRNAs and observed a decrease in mammary gland repopulation in Cbf-1 knockdown cells from Elf5-null MECs compared to control (Fig. 6I, 6J), further substantiating the in vitro observation. Taken together, our data confirm that increase in MaSCs in Elf5-depleted mammary gland is mediated in part by upregulating Notch signaling.

Discussion

In this study, we demonstrate that conditional ablation of Elf5 in mammary epithelium results in accumulation of a sizeably enriched population of $K14^{+}$ cells in the luminal compartment. These $K14^{+}$ cells are not misplaced myoepithelial cells; neither do they express differentiated markers of such cell types such as SMA. On the other hand, staining data suggest that these populations of cells in the Elf5-null mammary gland are double K14/K8 positive—a characteristic attributed to bipotential progenitor cells [24, 34]. It is worth noting that similar expansion of K8/K14 dual-positive cells have been reported in Par-3-depleted mammary glands and in a mouse model that expresses a chimeric protein consisting of ETV6 (an E-twenty six family transcription factor) and the protein tyrosine kinase domain of NTRK3 [35, 36]. Importantly, in both cases, the appearance of the K8/K14 dual-positive cells was accompanied by the accumulation of bipotential progenitor cells suggesting a possible causal link between these cell types. Finally, the notion that coexpression of markers associated with multiple lineages can infer developmental and cellular plasticity is further strengthened by a recent study on fetal MaSC populations, which coexpress K14 and K8 in the developing mouse mammary glands and in mammospheres [37].

The increase in $CD61^{+}$ luminal progenitors in Elf5-null pregnant mammary epithelium is not surprising and has indeed been reported before using mammary transplants [16]. However, what is interesting is the observation that a large fraction of the $CD61^{+}$ population coexpress K14 and K8 exclusively in the Elf5-null mammary epithelium (Fig. 3) suggesting that the $K14^{+}/K8^{+}$ dual population might represent the blocked $CD61^{+}$ progenitors. We also detect a similar increase in the $K14^{+}/K8^{+}$ dual population in $CD61^{+}$-sorted population from the virgin Elf5-null mammary glands (Fig. 4), albeit at a much lower frequency, suggesting that changes in this population might start earlier. These data reveal new insights into this important subclass of $CD61^{+}$ progenitor cells, which have been shown to represent cancer

stem cells that sustain specific mammary tumors [38]. Another novel and perhaps more interesting finding of our study is the significant increase in stem cell population (MaSC-enriched $Lin^{-}CD24^{+}CD29^{hi}$) in Elf5-null mammary epithelium, a phenotype not just restricted to the pregnant state but also detectable in virgin glands. The functional consequence of this increase in stem cell/luminal progenitors was clearly evident in results from mammosphere and colony-forming assays, which show increase in MaSC activity of the Elf5-Null MECs. Additional support came from in vivo transplantation assays, which demonstrated an increase in repopulation frequency in transplants from Elf5-null MECs compared to WT. These results are striking in the face of a previous report suggesting that Elf5-null MaSCs do not differ in their repopulating potential compared to their WT counterparts [16]. However, since the relevant data for such transplantation experiments were not presented, it is difficult to reconcile the discrepancy between these findings. We suspect that this difference might reflect the nature of the genetic system used to examine the loss of Elf5, that is, conditional knockout of Elf5 compared to mammary transplant studies or the effects of different mouse strains.

The transcriptome profiling of the Elf5-null mammary glands has offered new insights into possible molecular mechanisms to account for the altered stem/progenitor functions as exemplified by the observed changes in the Notch signaling pathway. Notch signaling influences a broad spectrum of cellular processes including stem cell maintenance and self-renewal, cell-fate decisions, and differentiation in a variety of tissues and organs including mammary glands [32, 39–41]. The biological effects of canonical Notch signaling are mediated through interactions between several Notch receptors and ligands, which leads to activation of Rbpjk/Cbf-1 and induction of downstream target gene expression [42]. A wealth of studies have implicated Notch signaling in controlling various aspects of stem/progenitor cell biology, such as their specification, maintenance, and differentiation in a variety of organs and tissues including mammary glands. For example, targeted disruption of Rbpjk/Cbf-1 in the mouse mammary gland during pregnancy results in progressive expansion of the basal cell population combined with a luminal to basal cell-fate switch [33]. In contrast, it has been shown that in human mammospheres in culture, activation of the Notch pathway, specifically Notch4, was critical for maintaining stem/progenitor cell activity and myoepithelial cell expansion [43]. Another recent study has demonstrated that activated Notch signaling promotes commitment of MaSCs to the luminal cell lineage and maintains them in an undifferentiated stage [32]. Given the high levels of Notch1 expression selectively in luminal populations, it is thought that this receptor might be the primary mediator that prods MaSCs toward luminal cell fate and promotes expansion and self-renewal and ultimately transformation of $CD61^{+}$ luminal progenitor cells [38].

One complicating aspect of Notch-related studies is the inherent complexity of multiple Notch receptors and ligands and their dynamic expression and activity during various stages of mammary gland development [44]. We have faced this dilemma during our studies. Indeed our results indicate that the changes in expression of specific Notch receptors, ligands, and downstream mediators depend to a large extent on the cellular, experimental, and developmental contexts (e.g., virgin vs. pregnant). Nevertheless, our data from Elf5-null mammary glands as well as isolated MECs clearly show activation of the canonical Notch pathway as evident by increased NICD1 and NICD4 and upregulation of key downstream

targets of Notch, such as Hes-1 and Hey-1. Importantly, the hyperactive Notch signaling in the Elf5 null MECs is of functional consequence since inhibition of the Notch signaling reverted the increased MaSC activity of these cells as evidenced by mammosphere, colony forming as well as in vivo transplantation assays (Fig. 6). Based on our recent chromatin immunoprecipitation experiments demonstrating that there are Elf5-responsive elements in the *Notch1* gene, we suspect that the increase in Notch1 levels is a direct consequence of the Elf5-loss [17]. It is tempting to speculate that the upregulation of Notch3 and Notch4 might also account, in part, for the increase in the MaSC-enriched $Lin^{-}CD24^{+}CD29^{hi}$ populations as has been suggested from human mammosphere studies [43, 45]. Future genetic studies wherein individual or combinations of Notch receptor are specifically ablated in the mammary gland will shed light on the relative contributions of individual Notch family members.

Overexpression of active forms of the Notch1 and Notch4 receptors transform both normal human and murine MECs [46, 47]. Furthermore, accumulation of NICD1 and increased Notch signaling are observed in human breast cancer samples [48]. Given the double-pronged assault of activated Notch signaling and increased MaSC-enriched and $CD61^{+}$ population in an Elf5-null background, we hypothesize that loss of Elf5 is likely to provide a fertile ground for tumor development. We posit that Elf5 might serve as a tumor suppressor gene in breast epithelium and that its loss could lead to dedifferentiation and expansion of potential tumor-initiating progenitor cells. This is an interesting and important area of future investigation that is currently underway in our laboratory.

Conclusions

In conclusion, our studies with Elf5 conditional knockout mice have unearthed a hitherto undescribed role of Elf5 in regulating MaSC activity. This novel function of Elf5 coupled with its well-characterized effects on the luminal progenitor population suggests that this transcription factor not only regulates various aspects of mammary gland development and differentiation but may also influence stem cell lineage choices and thus tumorigenesis. Finally, our discovery that hyperactivation of Notch pathway acts as a potent driver for the Elf5-null phenotype offers new mechanistic insights into this important signaling pathway.

Supplementary Material

Refer to Web version on PubMed Central for supplementary material.

Acknowledgments

We acknowledge the contribution of Dr. Yeon Sook Choi in the initial phase of these studies. We are especially grateful to Irene Kulik and Xiang Hang for excellent technical assistance. We thank Bong Ihn Koh and Mario Andres Blanco for helpful discussions. This research was supported by grants from R01GM069417 to S.S. and from the Brewster Foundation, the Champalimaud Foundation, the U. S. Department of Defense, and the National Institutes of Health (R01CA134519 and R01CA141062) to Y.K. R.C. is a recipient of a DOD postdoctoral fellowship (W81XWH-11-1-0681).

References

1. Watson CJ, Khaled WT. Mammary development in the embryo and adult: A journey of morphogenesis and commitment. Development. 2008; 135:995–1003. [PubMed: 18296651]
2. Hennighausen L, Robinson GW. Information networks in the mammary gland. Nat Rev Mol Cell Biol. 2005; 6:715–725. [PubMed: 16231422]
3. LaMarca HL, Rosen JM. Minireview: Hormones and mammary cell fate—What will I become when I grow up? Endocrinology. 2008; 149:4317–4321. [PubMed: 18556345]
4. Visvader JE. Keeping abreast of the mammary epithelial hierarchy and breast tumorigenesis. Genes Dev. 2009; 23:2563–2577. [PubMed: 19933147]
5. Siegel PM, Muller WJ. Transcription factor regulatory networks in mammary epithelial development and tumorigenesis. Oncogene. 2010; 29:2753–2759. [PubMed: 20348953]
6. Choi YS, Cheng J, Segre J, et al. Generation and analysis of Elf5-LacZ mouse: Unique and dynamic expression of Elf5 (ESE-2) in the inner root sheath of cycling hair follicles. Histochem Cell Biol. 2008; 129:85–94. [PubMed: 17938949]
7. Lapinskas EJ, Palmer J, Ricardo S, et al. A major site of expression of the ets transcription factor Elf5 is epithelia of exocrine glands. Histochem Cell Biol. 2004; 122:521–526. [PubMed: 15655699]
8. Metzger DE, Xu Y, Shannon JM. Elf5 is an epithelium-specific, fibroblast growth factor-sensitive transcription factor in the embryonic lung. Dev Dyn. 2007; 236:1175–1192. [PubMed: 17394208]
9. Oettgen P, Kas K, Dube A, et al. Characterization of ESE-2, a novel ESE-1-related Ets transcription factor that is restricted to glandular epithelium and differentiated keratinocytes. J Biol Chem. 1999; 274:29439–29452. [PubMed: 10506207]
10. Zhou J, Ng AY, Tymms MJ, et al. A novel transcription factor, elf5, belongs to the elf subfamily of ets genes and maps to human chromosome 11p13–15, a region subject to loh and rearrangement in human carcinoma cell lines. Oncogene. 1998; 17:2719–2732. [PubMed: 9840936]
11. Donnison M, Beaton A, Davey HW, et al. Loss of the extraembryonic ectoderm in Elf5 mutants leads to defects in embryonic patterning. Development. 2005; 132:2299–2308. [PubMed: 15829518]
12. Zhou J, Chehab R, Tkalcevic J, et al. Elf5 is essential for early embryogenesis and mammary gland development during pregnancy and lactation. EMBO J. 2005; 24:635–644. [PubMed: 15650748]
13. Ng RK, Dean W, Dawson C, et al. Epigenetic restriction of embryonic cell lineage fate by methylation of Elf5. Nat Cell Biol. 2008; 10:1280–1290. [PubMed: 18836439]
14. Choi YS, Chakrabarti R, Escamilla-Hernandez R, et al. Elf5 conditional knockout mice reveal its role as a master regulator in mammary alveolar development: Failure of Stat5 activation and functional differentiation in the absence of Elf5. Dev Biol. 2009; 329:227–241. [PubMed: 19269284]
15. Harris J, Stanford PM, Sutherland K, et al. Socs2 and elf5 mediate prolactin-induced mammary gland development. Mol Endocrinol. 2006; 20:1177–1187. [PubMed: 16469767]
16. Oakes SR, Naylor MJ, Asselin-Labat ML, et al. The Ets transcription factor Elf5 specifies mammary alveolar cell fate. Genes Dev. 2008; 22:581–586. [PubMed: 18316476]
17. Escamilla-Hernandez R, Chakrabarti R, Romano RA, et al. Genome-wide search identifies Ccnd2 as a direct transcriptional target of Elf5 in mouse mammary gland. BMC Mol Biol. 2010; 11:68. [PubMed: 20831799]
18. Rogers RL, Van Seuningen I, Gould J, et al. Transcript profiling of Elf5+/− mammary glands during pregnancy identifies novel targets of Elf5. PLoS One. 2010; 5:e13150. [PubMed: 20949099]
19. Asselin-Labat ML, Sutherland KD, Barker H, et al. Gata-3 is an essential regulator of mammary-gland morphogenesis and luminal-cell differentiation. Nat Cell Biol. 2007; 9:201–209. [PubMed: 17187062]
20. Kouros-Mehr H, Slorach EM, Sternlicht MD, et al. GATA-3 maintains the differentiation of the luminal cell fate in the mammary gland. Cell. 2006; 127:1041–1055. [PubMed: 17129787]

21. Lim E, Wu D, Pal B, et al. Transcriptome analyses of mouse and human mammary cell subpopulations reveal multiple conserved genes and pathways. Breast Cancer Res. 2010; 12:R21. [PubMed: 20346151]
22. Naylor MJ, Li N, Cheung J, et al. Ablation of beta1 integrin in mammary epithelium reveals a key role for integrin in glandular morphogenesis and differentiation. J Cell Biol. 2005; 171:717–728. [PubMed: 16301336]
23. Pei XH, Bai F, Smith MD, et al. CDK inhibitor p18(INK4c) is a downstream target of GATA3 and restrains mammary luminal progenitor cell proliferation and tumorigenesis. Cancer Cell. 2009; 15:389–401. [PubMed: 19411068]
24. Shackleton M, Vaillant F, Simpson KJ, et al. Generation of a functional mammary gland from a single stem cell. Nature. 2006; 439:84–88. [PubMed: 16397499]
25. Hu Y, Smyth GK. ELDA: Extreme limiting dilution analysis for comparing depleted and enriched populations in stem cell and other assays. J Immunol Methods. 2009; 347:70–78. [PubMed: 19567251]
26. Mootha VK, Lindgren CM, Eriksson KF, et al. PGC-1alpha-responsive genes involved in oxidative phosphorylation are coordinately downregulated in human diabetes. Nat Genet. 2003; 34:267–273. [PubMed: 12808457]
27. Subramanian A, Tamayo P, Mootha VK, et al. Gene set enrichment analysis: A knowledge-based approach for interpreting genome-wide expression profiles. Proc Natl Acad Sci USA. 2005; 102:15545–15550. [PubMed: 16199517]
28. Mikaelian I, Hovick M, Silva KA, et al. Expression of terminal differentiation proteins defines stages of mouse mammary gland development. Vet Pathol. 2006; 43:36–49. [PubMed: 16407485]
29. Sun P, Yuan Y, Li A, et al. Cytokeratin expression during mouse embryonic and early postnatal mammary gland development. Histochem Cell Biol. 2010; 133:213–221. [PubMed: 19937336]
30. Stingl J, Eirew P, Ricketson I, et al. Purification and unique properties of mammary epithelial stem cells. Nature. 2006; 439:993–997. [PubMed: 16395311]
31. Dontu G, Abdallah WM, Foley JM, et al. In vitro propagation and transcriptional profiling of human mammary stem/progenitor cells. Genes Dev. 2003; 17:1253–1270. [PubMed: 12756227]
32. Bouras T, Pal B, Vaillant F, et al. Notch signaling regulates mammary stem cell function and luminal cell-fate commitment. Cell Stem Cell. 2008; 3:429–441. [PubMed: 18940734]
33. Buono KD, Robinson GW, Martin C, et al. The canonical Notch/RBP-J signaling pathway controls the balance of cell lineages in mammary epithelium during pregnancy. Dev Biol. 2006; 293:565–580. [PubMed: 16581056]
34. Villadsen R, Fridriksdottir AJ, Ronnov-Jessen L, et al. Evidence for a stem cell hierarchy in the adult human breast. J Cell Biol. 2007; 177:87–101. [PubMed: 17420292]
35. Li Z, Tognon CE, Godinho FJ, et al. ETV6-NTRK3 fusion oncogene initiates breast cancer from committed mammary progenitors via activation of AP1 complex. Cancer Cell. 2007; 12:542–558. [PubMed: 18068631]
36. McCaffrey LM, Macara IG. The Par3/aPKC interaction is essential for end bud remodeling and progenitor differentiation during mammary gland morphogenesis. Genes Dev. 2009; 23:1450–1460. [PubMed: 19528321]
37. Spike BT, Engle DD, Lin JC, et al. A mammary stem cell population identified and characterized in late embryogenesis reveals similarities to human breast cancer. Cell Stem cell. 2012; 10:183–197. [PubMed: 22305568]
38. Vaillant F, Asselin-Labat ML, Shackleton M, et al. The mammary progenitor marker CD61/beta3 integrin identifies cancer stem cells in mouse models of mammary tumorigenesis. Cancer Res. 2008; 68:7711–7717. [PubMed: 18829523]
39. Chiba S. Notch signaling in stem cell systems. Stem Cells. 2006; 24:2437–2447. [PubMed: 16888285]
40. Farnie G, Clarke RB. Mammary stem cells and breast cancer—Role of Notch signalling. Stem Cell Rev. 2007; 3:169–175. [PubMed: 17873349]
41. Raouf A, Zhao Y, To K, et al. Transcriptome analysis of the normal human mammary cell commitment and differentiation process. Cell Stem Cell. 2008; 3:109–118. [PubMed: 18593563]

42. Kopan R, Ilagan MX. The canonical Notch signaling pathway: Unfolding the activation mechanism. Cell. 2009; 137:216–233. [PubMed: 19379690]

43. Dontu G, Jackson KW, McNicholas E, et al. Role of Notch signaling in cell-fate determination of human mammary stem/progenitor cells. Breast Cancer Res. 2004; 6:R605–R615. [PubMed: 15535842]

44. Raafat A, Goldhar AS, Klauzinska M, et al. Expression of Notch receptors, ligands, and target genes during development of the mouse mammary gland. J Cell Physiol. 2011; 226:1940–1952. [PubMed: 21506125]

45. Sansone P, Storci G, Giovannini C, et al. p66Shc/Notch-3 interplay controls self-renewal and hypoxia survival in human stem/progenitor cells of the mammary gland expanded in vitro as mammospheres. Stem Cells. 2007; 25:807–815. [PubMed: 17158237]

46. Dievart A, Beaulieu N, Jolicoeur P. Involvement of Notch1 in the development of mouse mammary tumors. Oncogene. 1999; 18:5973–5981. [PubMed: 10557086]

47. Imatani A, Callahan R. Identification of a novel NOTCH-4/INT-3 RNA species encoding an activated gene product in certain human tumor cell lines. Oncogene. 2000; 19:223–231. [PubMed: 10645000]

48. Stylianou S, Clarke RB, Brennan K. Aberrant activation of notch signaling in human breast cancer. Cancer Res. 2006; 66:1517–1525. [PubMed: 16452208]

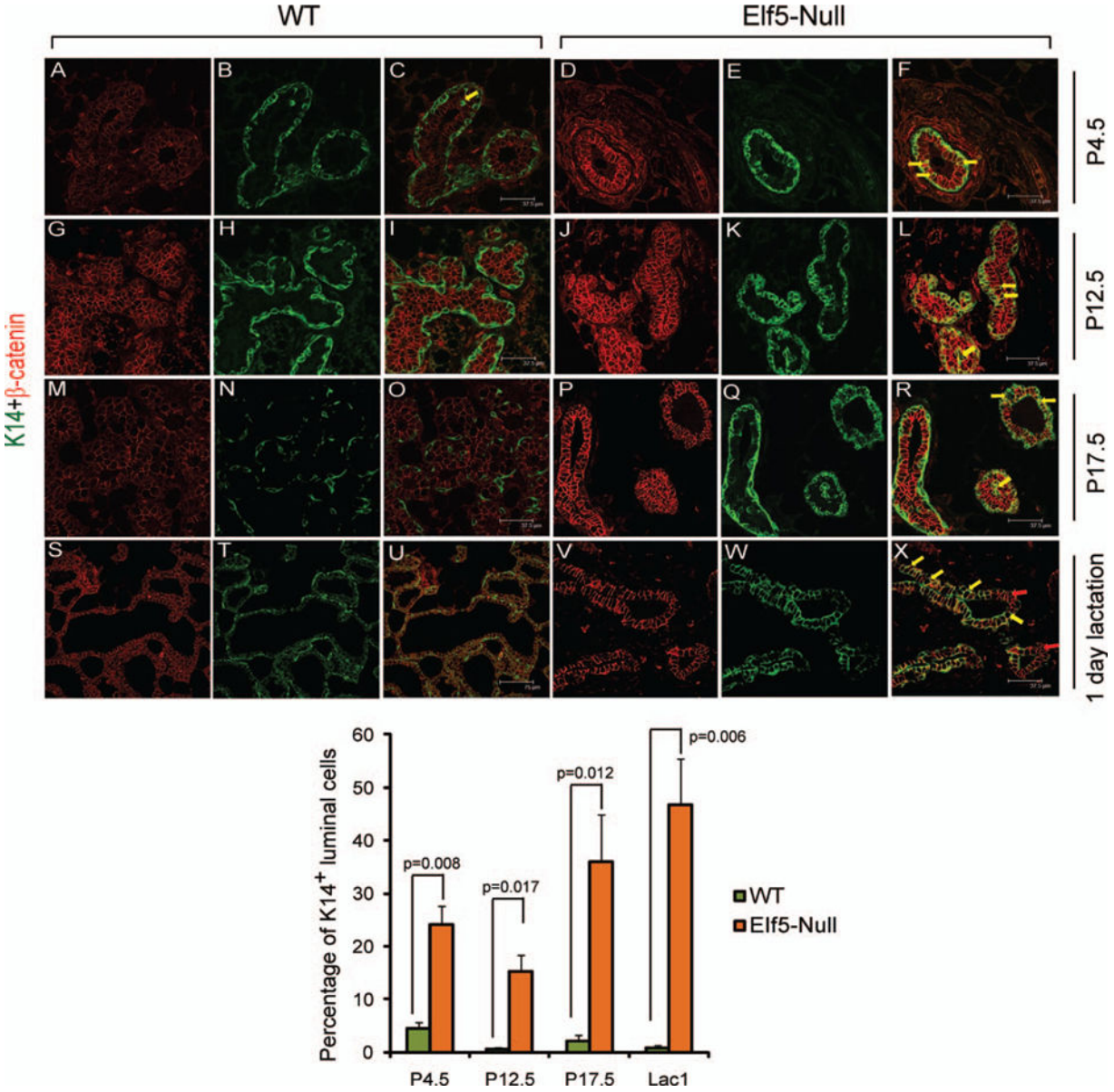

Figure 1.

Altered expression of K14 during pregnancy. (**A–F**): P4.5, (**G–L**) P12.5, (**M–R**) P17.5, and (**S–X**) L1. At P4.5d, in WT tissues, K14 was expressed exclusively at the basal cells. Occasional K14 cells were present in luminal compartment as shown by yellow arrow (C). However, in P4.5 Elf5-null tissue, cells were frequently observed in luminal compartment that were positive for K14 (yellow arrows in F). At later time points during pregnancy and lactation (P12.5d-L1), K14 was expressed exclusively at the basal cells as in (I), (O), and (U) in the WT tissue. In Elf5-null tissues, large numbers of K14-positive cells were observed in the luminal compartment of the mammary epithelium (L, R). Yellow arrows indicate aberrant localization of K14 in luminal compartment and red arrows indicate the unaffected normal luminal cells negative for K14 at term (X). Bar graph below represents quantification of percentage $K14^+$ population in the luminal compartment. Data represent mean ± SD of

average of 10 image fields from six animals per genotype, *p* values calculated by *t* test for statistical significance. Abbreviations: Elf5, E74-like factor 5; WT, wild-type.

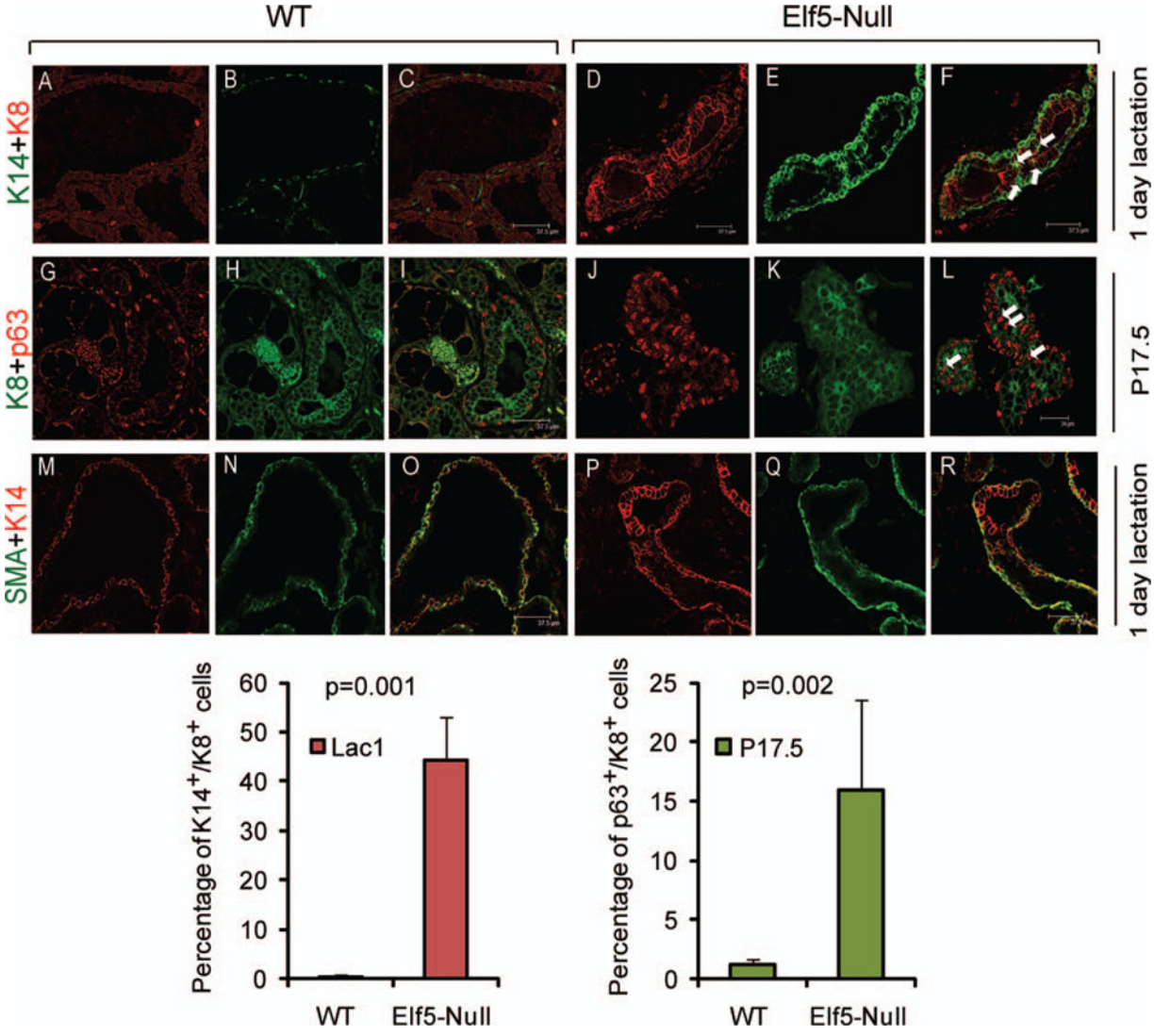

Figure 2.

Colocalization of K14/p63 and K8 in luminal compartment during pregnancy. (**A–F**): L1, (**G–L**) P17.5, and (**M–R**) L1. Expression of K14 and p63 is present exclusively in basal compartment in WT tissue (C, I). However, in Elf5-null tissue, an increase in double-positive $K14^+/K8^+$ was observed as shown by white arrows (F). In some areas, almost all cells in mammary epithelium were positive for K14 and K8, particularly at parturition as shown by white arrows. (L) Increase in $K8^+/p63^+$ dual-positive cells was observed in Elf5-null mammary gland (white arrows in L). $K14^+$ cells in the luminal compartment are negative for smooth muscle actin (SMA) (O and R). Altered localization of K14 was observed in the luminal compartment (columnar cells) in Elf5-null mammary epithelium (R) in comparison to WT tissues, where K14 was expressed predominantly at the basal cells (O). Note: SMA staining is absent in the luminal compartment and is present only in the basal cells in both WT and Elf5-null mammary epithelium. Bar graph below represents quantification of percentage $K14^+/K8^+$ population (left) and $p63^+/K8^+$ population (right) in the mammary epithelium. Data represent mean ± SD of average of six images from 4 to 6

animals per genotype, *p* values calculated by *t* test for statistical significance. Abbreviations: Elf5, E74-like factor 5; WT, wild-type.

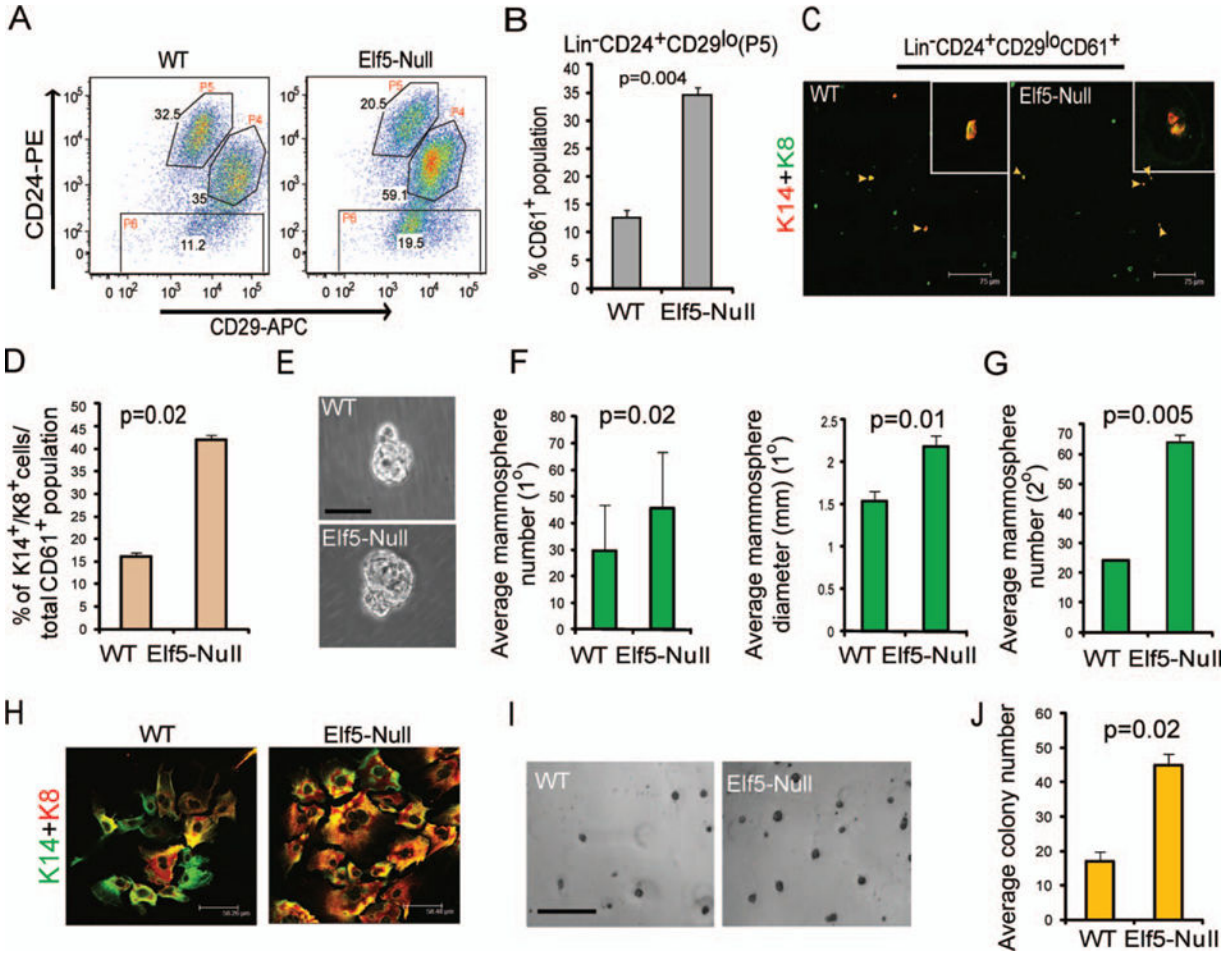

Figure 3.

Elf5 loss leads to expansion of stem/progenitor population activity and increase in K14/K8 double-positive cells in CD61$^+$ subpopulations during pregnancy. Mammary epithelial cells (MECs) were isolated and analyzed by flow cytometry for Lin$^-$CD24$^+$CD29^{hi} (P4) and Lin$^-$CD24$^+$CD29^{lo} (P5) populations from WT and Elf5-null mammary gland at P17.5. Independent experiments were repeated with five animals per genotype (**A**). (**B**): Bar graph depicting the percentage of CD61$^+$ progenitor population from Lin$^-$CD24$^+$CD29^{lo} (P5) population of Elf5-null MECs in comparison to WT from P17.5. Data represent mean ± SD of three independent experiments, *p* values calculated by *t* test. (**C**): Analysis of immunofluorescence data show increased K14$^+$/K8$^+$ cells in CD61$^+$-sorted subpopulations from P5 of P17.5 Elf5-null MECs in comparison to WT (as shown by yellow arrowheads). Insets show higher magnification. (**D**): Bar graphs represent quantification of K14$^+$/K8$^+$ double-positive cells. Four animals per genotype were examined and *p* values were calculated by *t* test for statistical significance. (**E**): MECs from WT and Elf5-null mice mammary gland at P17.5d were analyzed for mammosphere assay. Ten thousand cells per milliliter (total, 2 ml) were grown as described in Methods and Materials and photographed and counted after 7 days. Representative mammospheres are shown in (E) scale bar = 20 μm. Bar graphs (**F**) show quantification of mammosphere numbers and diameter (in mm), respectively. Bar graphs represent the mean ± SD of triplicates of three animals each group.

(**G**): Second-generation mammospheres were grown as described in Methods and Materials and counted. Bar graph represents the mean 6 SD of duplicates of two animals each group. (**H**): Differentiated mammospheres on collagen stained with K14 and K8. (**I**): Freshly isolated MECs from P17.5 were seeded at clonal density of 1,000 cells in Matrigel-coated 24-well plate. Colonies were photographed and counted 9 days after culture. Representative spherical colonies are shown in scale bar = 100 μm. (**J**): Quantification of colony numbers as shown by bar graph. Bar graph represents the mean ± SD of three animals per group and each sample was examined in triplicate. Abbreviations: Elf5, E74-like factor 5; WT, wild-type.

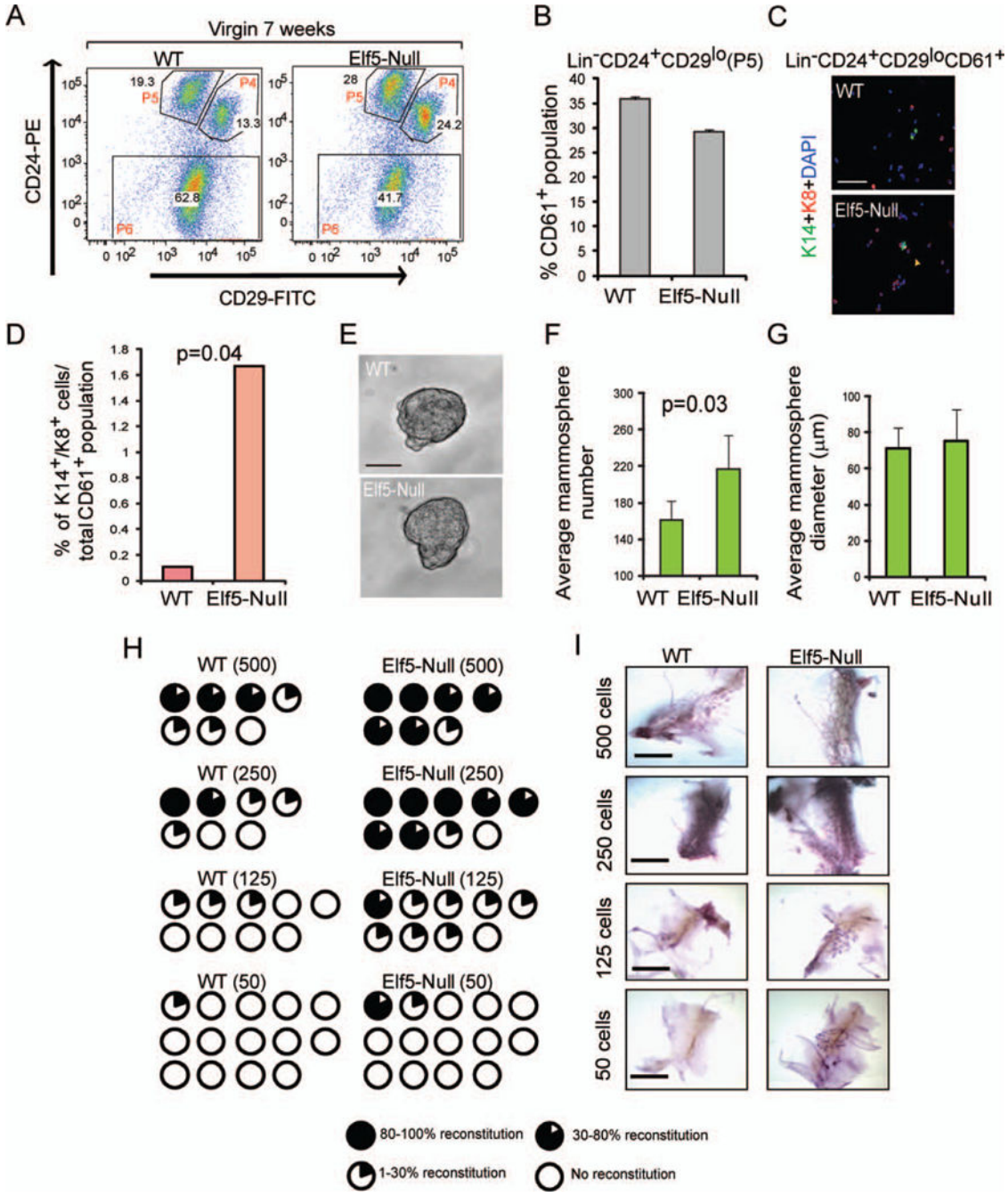

Figure 4.

Increased stem/progenitor cell population and activity in Elf5-null MECs from virgin animals. (**A**): Mammary epithelial cells (MECs) were isolated and analyzed by flow cytometry for $Lin^{-}CD24^{+}CD29^{hi}$ (P4) and $Lin^{-}CD24^{+}CD29^{lo}$ (P5) populations from WT and Elf5-null mammary gland at 7 weeks virgin time point. Independent experiments were repeated with 4 WT and 6 Elf5-null animals per genotype, respectively. (**B**): Bar graph depicting the percentage of $CD61^{+}$ progenitor population from P5 population of Elf5-null MECs in comparison to WT from 7-week virgin MECs. (**C**): Analysis of

immunofluorescence data shows increased $K14^+/K8^+$ cells in $CD61^+$ subpopulations from Elf5-null MECs in comparison to WT (as shown by yellow arrowhead). Scale bar in C = 100 μm. (**D**): Bar graphs represent quantification of $K14^+/K8^+$ double-positive cells. (**E**): Representative mammospheres from 7-week virgin mammary epithelium of WT versus Elf5-null animal. Scale bar in (E) = 40 μm. Bar graphs (**F, G**) show quantification of mammosphere numbers and diameter (μm), respectively. Bar graph represents the mean 6 SD of duplicates of two WT and four Elf5-null animals each group. *p* values were tested using *t* test for statistical significance. (**H**): WT and Elf5-null cells were FACS sorted with the Lin, CD24, and CD29 markers and injected into cleared mammary fat pads. The outgrowths were analyzed at 6–8 weeks post-transplantation. Number of cells of each population injected into each fat pad, the total number of fat pads injected, number of transplants that generated epithelial outgrowths, and the percentage of outgrowth occupancy described in Table 1. The extent to which each outgrowth filled the host fat pad is indicated graphically. Each circle represents one mammary gland; the blackened region represents the area filled with outgrowth. (**I**): Representative images from limiting dilution transplantations, scale bar = 2 mm. Abbreviations: DAPI, 4′, 6-diamidino-2-phenylindole; Elf5, E74-like factor 5; WT, wild-type.

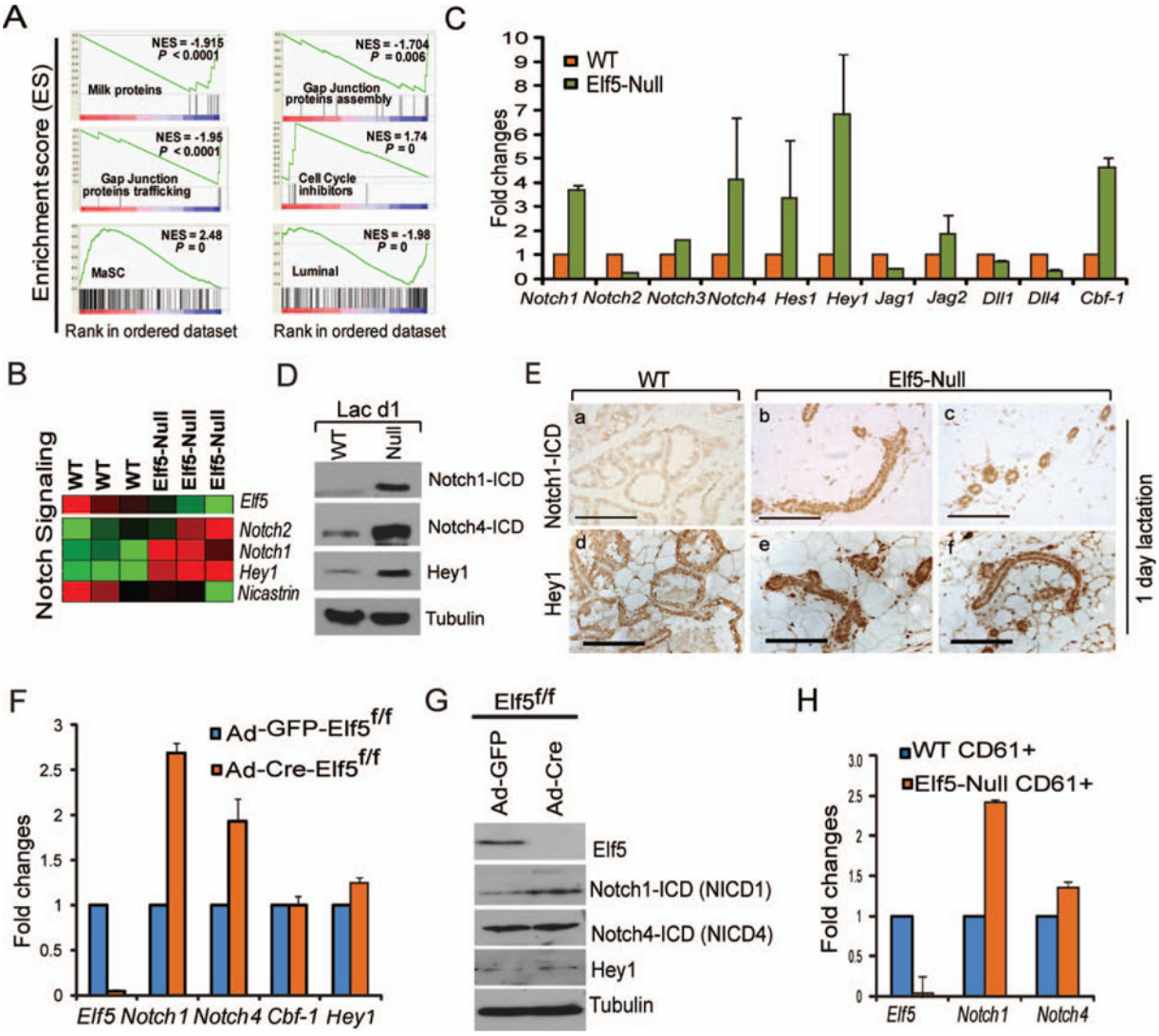

Figure 5.

Altered Notch pathway activation in Elf5-null mammary epithelium. (**A**): Gene-set enrichment analysis demonstrated reduction of milk protein gene signatures and gap junction protein genes in Elf5-null mammary epithelial cells (MECs) compared to WT. CDK inhibitors and MaSC-enriched genes are significantly overrepresented among upregulated genes in Elf5-null mammary gland transcriptome compared to WT. Luminal-enriched genes are significantly downregulated in Elf5-null mammary gland transcriptome compared to WT. (**B**): Heat map demonstrating upregulation of Notch signaling pathway in Elf5-null compared to WT. (**C**): Gene expression analysis of mammary glands from WT or Elf5-null mice at parturition. Real-time RT-PCR assays were performed in at least three independent experiments using three tissue samples. Real-time values normalized to house-keeping gene (*Gapdh*). Data are presented as the mean ± SD. (**D**): Western blot analysis of mammary gland extracts using anti-NICD1, anti-NICD4, and anti-Hey1 antibodies. Tubulin was used as loading control. (**E**): Immunostaining of mouse mammary epithelium with anti-NICD (A–C) shows high expression of NICD1 (B, C) in Elf5-null compared to WT mammary

epithelium that showed very weak to no expression of NICD1 (A). Immunostaining of mouse mammary epithelium with anti-Hey1 (D–F) shows increased expression of Hey1 in Elf5-null epithelium compared to WT-type mammary gland sections. Scale bar (E [A–C]) = 20 μm, (E [D–F]) = 40 μm. (**F**): Gene expression analysis of MECs from control (Ad-GFP-Elf5$^{f/f}$) and Elf5$^{f/f}$ mice transduced with Ad-Cre (Ad-Cre-Elf5$^{f/f}$) at 72 hours. The quantitative real-time assays were performed in duplicate using two independently generated samples. Real-time values normalized to house-keeping gene (*Gapdh*). In the absence of *Elf5*, *Notch1* and *Notch4* were upregulated. Changes in *Rbpjk/Cbf-1* and *Hey1* levels were not statistically significant. Data are represented as the mean ± SD. (**G**): Western blot analysis of protein lysates from Elf5$^{f/f}$ MECs transduced with Ad-Cre resulted in increased Notch activity (NICD1) in comparison to control MECs from Ad-GFP-Elf5$^{f/f}$. No significant change in expression in Notch4 activity or Hey1 was observed. Elf5 expression was knocked down in Ad-Cre/Elf5$^{f/f}$ MECs. (**H**): Increased expression of *Notch1* in CD61^{+}-sorted subpopulation from Elf5-null MECs in comparison to WT control. Note: *Elf5* was significantly downregulated in Elf5-null MECs. Bar graphs represent the mean ± SD of duplicates of two animals. Abbreviations: Elf5, E74-like factor 5; NES, normalized enrichment score; WT, wild-type.

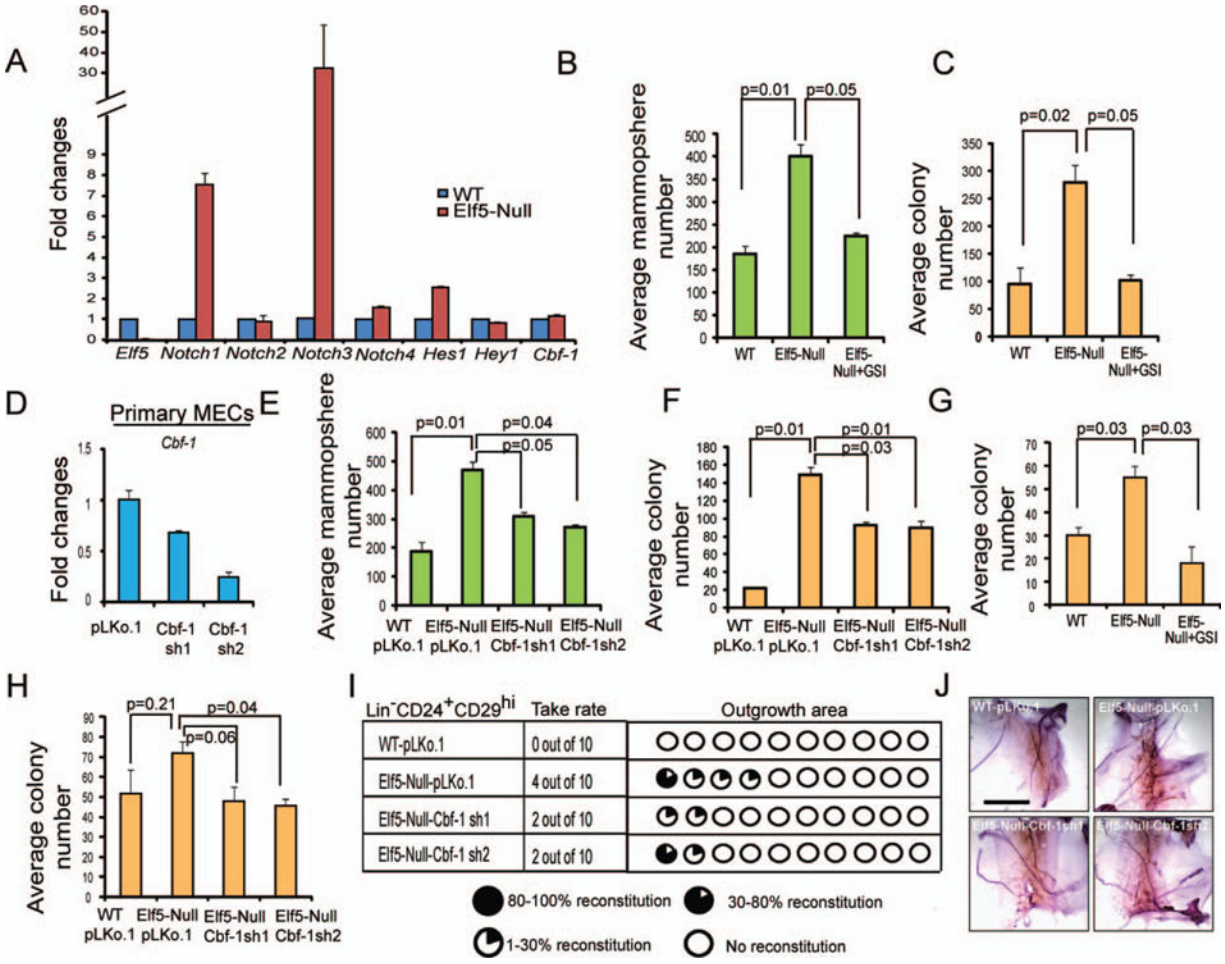

Figure 6.

The increased stem/progenitor cell phenotype of Elf5-null MECs can be rescued by attenuation of Notch activity. (**A**): Gene expression analysis of mammary glands from WT or Elf5-null mice at 6–8 weeks virgin. Real-time RT-PCR assays were performed in at least three independent experiments using three tissue samples. Real-time values normalized to house-keeping gene (*Gapdh*). Data are presented as the mean ± SD. (**B**): MECs from WT and Elf5-null mice mammary gland at 6 weeks virgin were freshly isolated and analyzed for mammosphere assay. Ten thousand cells per milliliter (total, 2 ml) were grown. Bar graph showing the number of mammospheres formed from WT and Elf5-null MECs treated with 4 μM GSI (MRK003) for 9 days. Data represent mean ± SD of two independent experiments. (**C**): MECs from WT and Elf5-null mice mammary gland at 6 weeks virgin were freshly isolated and analyzed for colony-forming assay (20, 000 cells per well) [24]. Bar graphs show quantification of colony numbers. Bar graphs represent the mean ± SD of duplicates of 2–3 animals each group. (**D**): Reduced Cbf-1 mRNA in MECs transduced with two independent Cbf-1-shRNAs (Cbf-1 sh1 and Cbf-1 sh2) compared to control as demonstrated by qRT-PCR. Data normalized to Gapdh. Data represent mean ± SD of two independent experiments. (**E, F**): Bar graphs show quantification of mammospheres (E) and colony numbers (F) from MECs transduced with either control or Cbf-1 shRNAs. (**G, H**): Freshly isolated and sorted $Lin^{-}CD24^{+}CD29^{hi}$ subpopulation from WT and Elf5-null mammary

gland at 6–8 week virgin was analyzed for colony formation with GSI treatment (G) or with Cbf-1 shRNAs transduction (H). (**I**): Sorted $Lin^{-}CD24^{+}CD29^{hi}$ subpopulations from WT and Elf5-null cells (100 cells per transplant) were injected into cleared mammary fat pads. The outgrowths were analyzed at 6–8 weeks post-transplantation for number of transplants that generated epithelial outgrowths (take rate). (**J**): Representative images from (I), scale bar = 2 mm. Abbreviations: Elf5, E74-like factor 5; GSI, gamma secretase inhibitor; MEC, mammary epithelial cell; WT, wild-type.

Table 1

Limiting dilution assay from WT and Elf5-null $Lin^{-}CD24^{+}CD29^{hi}$ cells

Number of cells injected/mammary fat pad	WT ($Lin^{-}CD24^{+}CD29^{hi}$) Number of outgrowths	Elf5-Null ($Lin^{-}CD24^{+}CD29^{hi}$) Number of outgrowths	WT ($Lin^{-}CD24^{+}CD29^{hi}$) Percentage of fat pad filled	Elf5-Null ($Lin^{-}CD24^{+}CD29^{hi}$) Percentage of fat pad filled
500	6/7	7/7	46.6% ± 18.6% (n = 6)	78.33% ± 21.3% (n = 7)
250	5/7	8/9	41.2% ± 20.6% (n = 5)	72.5% ± 15.05% (n = 8)
125	3/9	8/9	18.3% ± 12.5% (n = 3)	26.8% ± 21.7% (n = 8)
50	1/14	2/14	10% ± ND (n = 1)	35.0% ± 35% (n = 2)
Repopulating frequency (95% interval)	1/214	1/90	p value = .0042	
p value = .0123	(1/281-1/367)	(1/114-1/145)		

Transplantation of limiting numbers of $Lin^{-}CD24^{+}CD29^{hi}$ cells into cleared mammary fat pads revealed a ~2.4-fold increase in the absolute number of repopulating cells (p value = .0123) in the glands from Elf5-null mammary epithelial cellMECs compared to WT controls. Two-way ANOVA test showed significant differences (p value = .0042) observed in the extent of the fat pad occupation between WT and Elf5-null transplants.

Abbreviations: Elf5, E74-like factor 5; WT, wild-type. Abbreviations: El; ANOVA, analysis of variance.